CEDAR 2016

PLAN-OS

Electrodynamics of the Martian dynamo region near magnetic cusps and loops

J. A. Riousset,[1] C. S. Paty,[2] R. J. Lillis,[3] M. O. Fillingim,[3] S. L. England,[3] P. G. Withers,[4] and J. P. M. Hale[2]

[1]Physical Sciences Department, Embry-Riddle Aeronautical University, Daytona Beach, FL (jeremy.riousset@erau.edu)

[2]School of Earth and Atmospheric Sciences, Georgia Tech, Atlanta, GA; [3]Space Sciences Lab, UC Berkeley, Berkeley, CA; [4]Astronomy Department, Boston University, Boston, MA

Abstract

Strong and inhomogeneous remanent magnetization on Mars results in a complex pattern of crustal magnetic fields. The geometry and topology of these fields lead to atmospheric electrodynamic structures that are unique among the bodies of the solar system. In the atmospheric dynamo region (∼100–250 km altitude), ions depart from the gyropath due to collisions with neutral particles, while electron motion remains governed by electromagnetic drift. This differential motion of the charge carriers generates electric currents, which induce a perturbation field. The electromagnetic changes ultimately alter the behavior of the local ionosphere beyond the dynamo region. Here we use multifluid modeling to investigate the dynamics around an isolated magnetic cusp and around magnetic loops or arcades representative of the magnetic topology near, for example, Terra Sirenum. Our results show consistent, circular patterns in the electric current around regions with high local field strength, with possible consequences on atmospheric escape of charged particles.

I. Introduction

Martian Crustal Fields

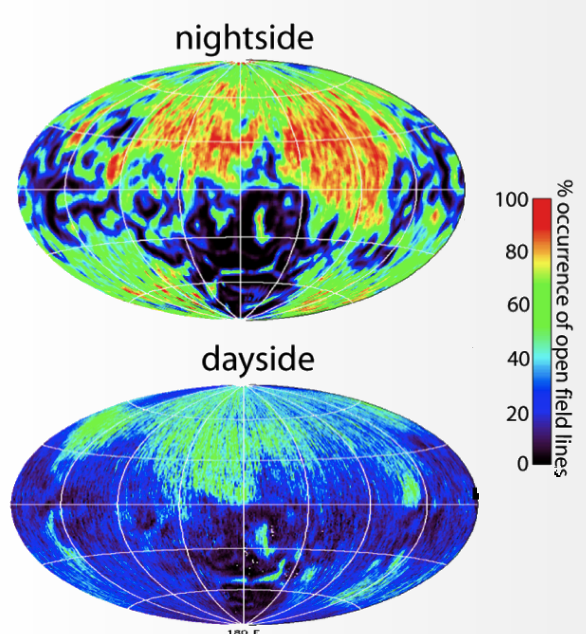

Figure 1: Percent occurrence of open field lines (i.e., connecting the IMF to the Martian atmosphere) at ∼400 km on the night- (top) and dayside (bottom) [*Brain et al.*, 2007].

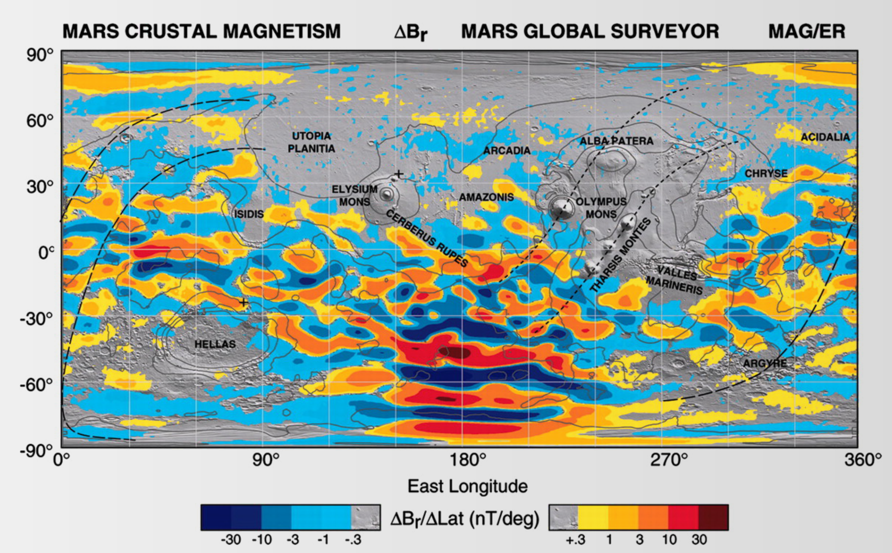

Figure 2: Martian magnetic field observed by MGS at 400 km altitude [*Connerney et al.*, 2005].

- Complex magnetic field configuration from remanent crustal fields with:
  - ↳ open/closed magnetic loop;
  - ↳ strong/weak magnetic field magnitude;
- Day-/nighttime asymmetry w.r.t. the solar wind interaction.

Dynamo Region

Definition: A **dynamo current** is generated by differential motions of positive and negative species:
↳ positive ions → governed by collisions with atmospheric wind-driven neutral particles (demagnetized);
↳ electrons → governed by gyromotion (magnetized).

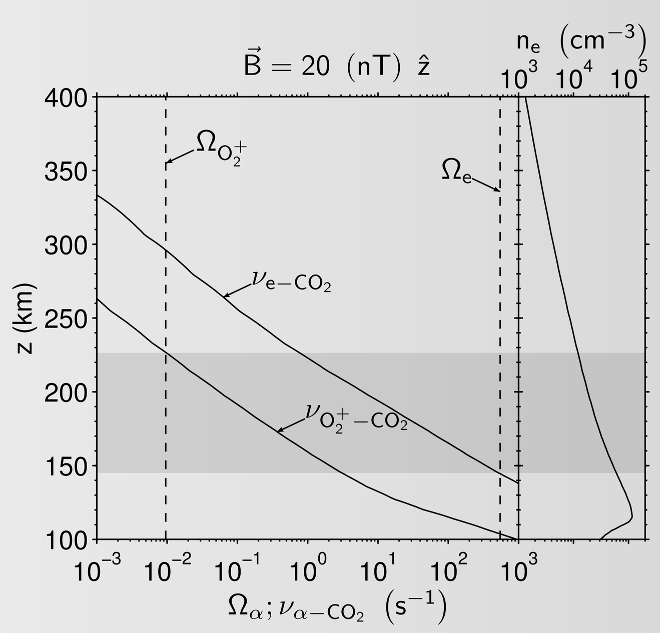

Figure 3: ▶ Estimated altitude of the dynamo region for a uniform, vertical magnetic field of magnitude 20 nT. Left hand side: electron-CO_2 collision frequency ν_{e-CO_2}, electron cyclotron frequency Ω_e, O_2^+–CO_2 collision frequency $\nu_{O_2^+-CO_2}$, and O_2^+ cyclotron frequency $\Omega_{O_2^+}$. Right hand side: vertical electron density profile. Gray shading: *a priori* altitude of the dynamo region.

$z \gtrsim 225$ km	$\nu_{O_2^+-CO_2} \ll \Omega_{CO_2}$ $\nu_{e-CO_2} \ll \Omega_e$	Magnetized ions Magnetized electrons	⇒ No dynamo current
150 km $\lesssim z \lesssim$ 225 km	$\nu_{O_2^+-CO_2} \gtrsim \Omega_{CO_2}$ $\nu_{e-CO_2} \ll \Omega_e$	Demagnetized ions Magnetized electrons	⇒ Ionospheric current
$z \lesssim 150$ km	$\nu_{O_2^+-CO_2} \gtrsim \Omega_{CO_2}$ $\nu_{e-CO_2} \gtrsim \Omega_e$	Demagnetized ions Demagnetized electrons	⇒ No differential current

Table 1: Drivers of the charged particle dynamics in the Martian ionosphere.

Transient Ionospheric Layers

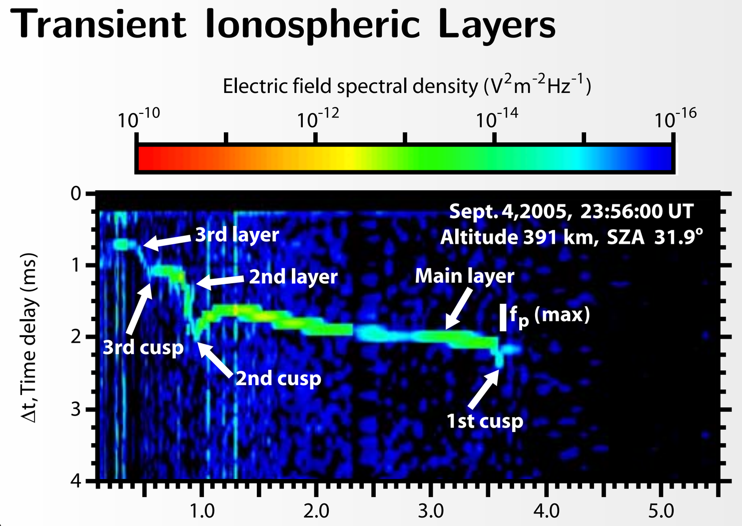

Figure 4: ◀ Ionogram with the characteristic signatures of the second, transient layer and a third topside layer [*Kopf et al.*, 2008].

- Location: dayside (more frequent at subsolar point than at terminator);
- Altitude: 180–220 km;
- Horizontal dimensions: 10–100+ km;
- Vertical thickness: a few 10s km;
- Timescale: tens of seconds to several minutes.

II. Model Formulation

The M[4] approach [*Riousset et al.*, 2013]:
- **M**ars (CO_2, & O);
- **M**ultifluid (O_2^+, CO_2^+, O^+, & e);
- **M**agnetoHydroDynamic (MHD);
- **M**odel.

(ℋ) **Hypotheses**
- No displacement current: $\varepsilon_0 \frac{\partial \vec{E}}{\partial t} \approx 0$;
- Massless electron: $m_e \approx 0$;
- Plasma approximation;
- Chemical equilibrium.

$$\frac{\partial n_i}{\partial t} = -\nabla \cdot \left(n_i \vec{V}_i\right)$$
$$\frac{\partial P_i}{\partial t} = -\nabla \cdot \left(P_i \vec{V}_i\right) + (\gamma - 1)\vec{V}_i \cdot \nabla P_i$$
$$\rho_i \frac{\partial \vec{V}_i}{\partial t} = -\rho_i \left(\vec{V}_i \cdot \nabla\right)\vec{V}_i + q_i n_i \left(\vec{E} + \vec{V}_i \times \vec{B}\right) - \nabla P_i - \frac{\rho_i G M_M}{(R_M + r)^2}\hat{r} + \sum_n \rho_i \nu_{i-n}\left(\vec{U}_n - \vec{V}_i\right)$$
$$\frac{\partial \vec{B}}{\partial t} = -\nabla \times \vec{E}$$
$$\vec{J} = \frac{\nabla \times \vec{B}}{\mu_0}$$

$$n_e = \sum_i n_i$$
$$\frac{\partial P_e}{\partial t} = -\nabla \cdot \left(P_e \vec{V}_e\right) + (\gamma - 1)\vec{V}_e \cdot \nabla P_e$$
$$\vec{V}_e = \sum_i \frac{n_i \vec{V}_i}{n_e} - \frac{\vec{J}}{e n_e}$$
$$\vec{E} = \frac{\vec{J} \times \vec{B}}{e n_e} - \sum_i \frac{n_i \vec{V}_i \times \vec{B}}{n_e} - \frac{\nabla P_e}{e n_e} + \frac{m_e}{e}\sum_n \nu_{n-e}\left(\vec{U}_n - \vec{V}_e\right)$$

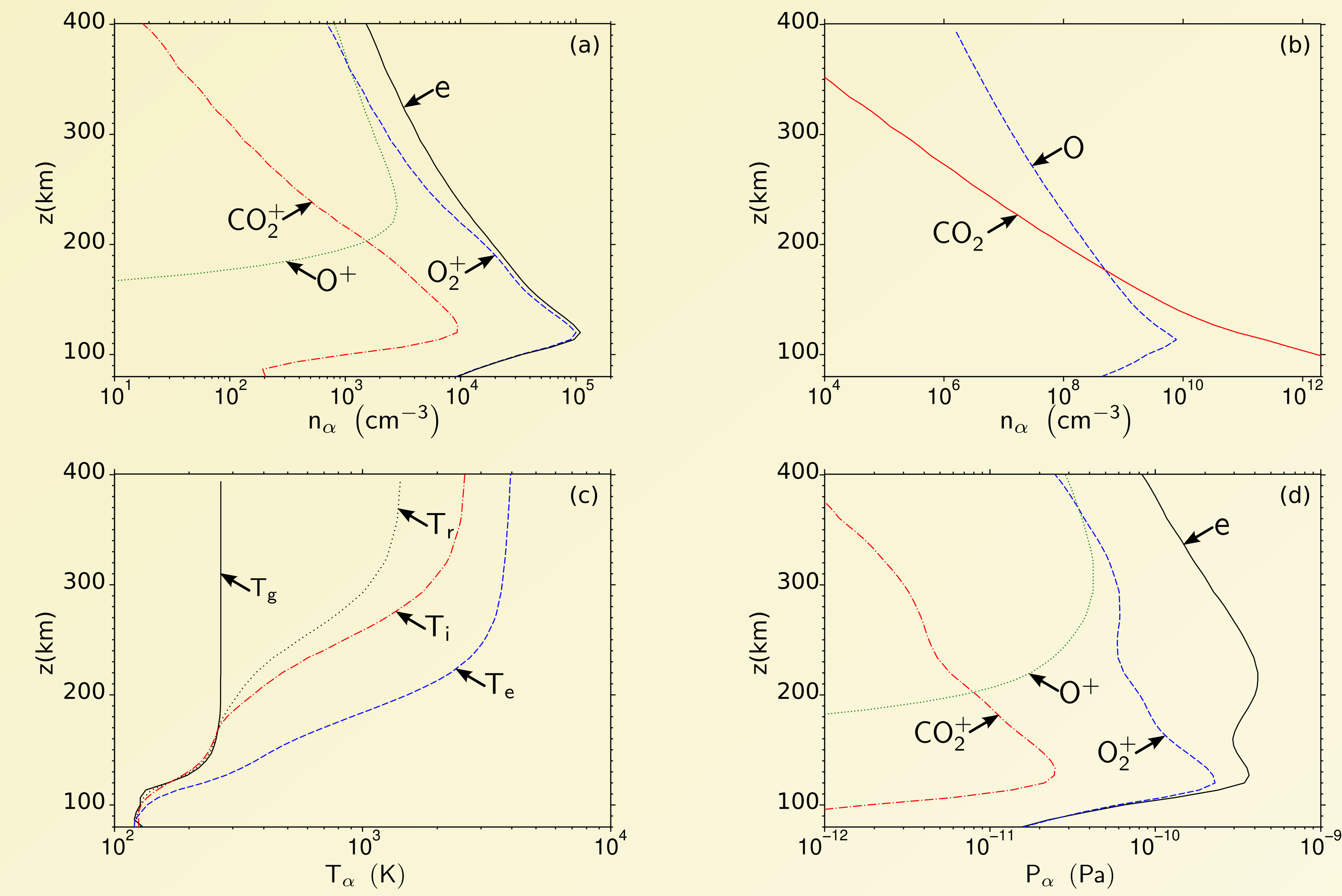

Figure 5: ▶ Initial profiles used for the simulation runs. The pressure for each species α is calculated as $p_\alpha = n_\alpha k_B T_\alpha$.

III. Results & Discussion

Magnetic Cusp

- Analog to structures at (15°N;15°E) & (10°S;110°E);
- Building block for complex structures (loops, arcades).

- Isolated dipole;
- Upward, buried @ −20 km;
- Magnetic moment: $\vec{\mu} = 10^{16}\,\mathrm{A \cdot m^2}\,\hat{z}$.

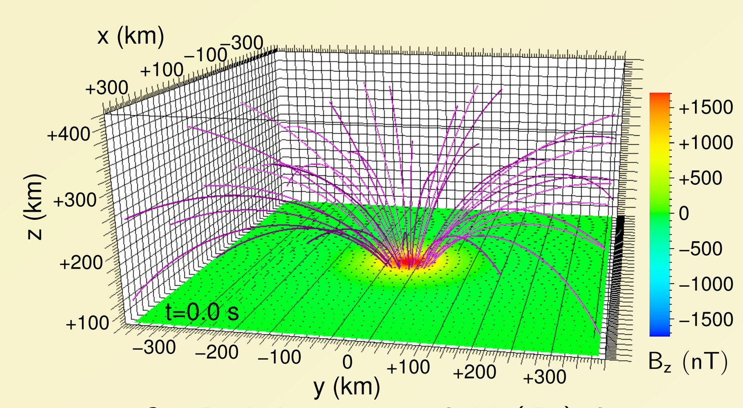

Figure 6: Radial magnetic field (B_z) for a cusp configuration. Solid magenta lines: magnetic field lines.

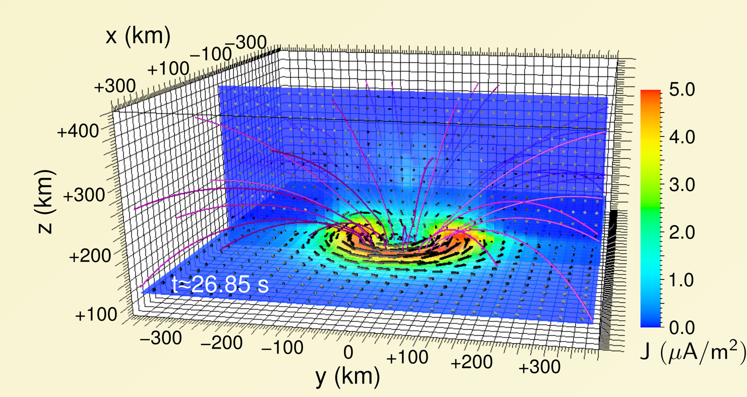

Figure 7: Magnitude (color map) and direction (solid black arrows) of the current density $\vec{J}$ in the planes y=0 km, and z=112 km. Solid magenta lines: magnetic field lines.

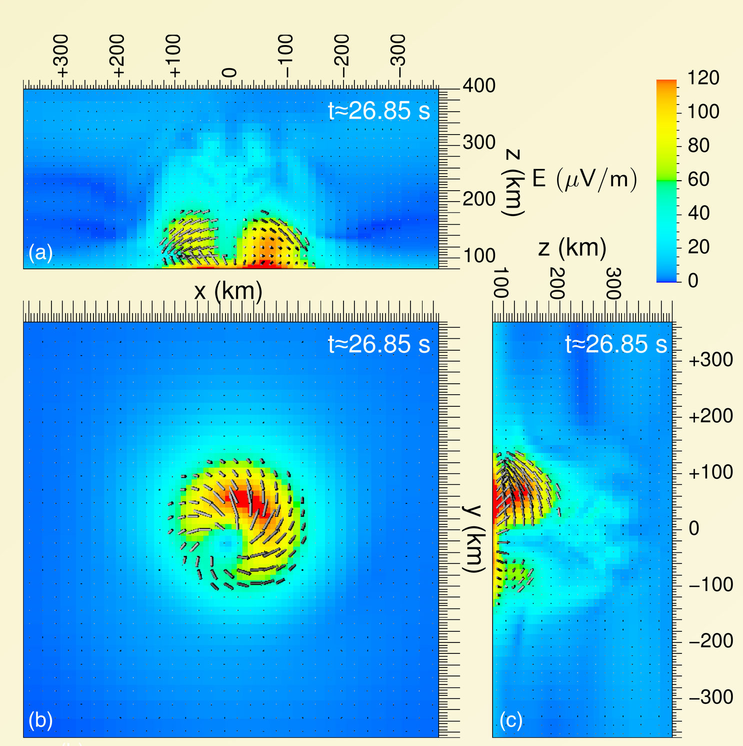

Figure 8: ◀ Magnitude (color map) and direction (solid arrows) of the electric field $\vec{E}$ in three cut planes: (a) y=0 km; (b) x=0 km; and (c) z=112 km (horizontal plane in the dynamo region).

$\vec{E}_\alpha$	Direction of $\vec{E}_\alpha$
$\vec{E}_1 = \frac{\vec{J} \times \vec{B}}{e n_e}$	$-\hat{z}$ & outward directed from the cusp
$\vec{E}_2 = -\sum_i \frac{n_i \vec{V}_i \times \vec{B}}{n_e}$	$+\hat{y}$ & $\begin{cases} +\hat{z}, & y \leq 0 \\ -\hat{z}, & y \geq 0 \end{cases}$
$\vec{E}_3 = -\frac{\nabla P_e}{e n_e}$	$\begin{cases} -\hat{z}, & z \leq 30\,\text{km} \\ +\hat{z}, & 130 \leq z \leq 160\,\text{km} \end{cases}$
$\vec{E}_4 = \frac{m_e}{e}\sum_{t=i,n} \nu_{te}\left(\vec{V}_t - \vec{V}_e\right)$	$\begin{cases} \simeq \vec{0} & \text{away from the cusp} \\ \text{horizontal, CCW else} \end{cases}$

- Ions are deviated into the neutral wind direction by collisions;
- Counterclockwise (CCW), torus-shaped current forms in dynamo region due to $\vec{E} \times \vec{B}$-drift of electrons.

Magnetic Arcades

- Superposition of isolated buried magnetic dipoles;
- Analog to Terra Sirenum magnetic topology.

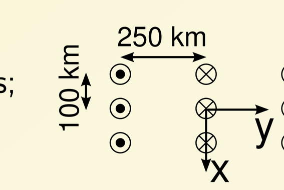

Figure 9: ◀ Sketch of the dipole setup yielding the magnetic arcade configuration.

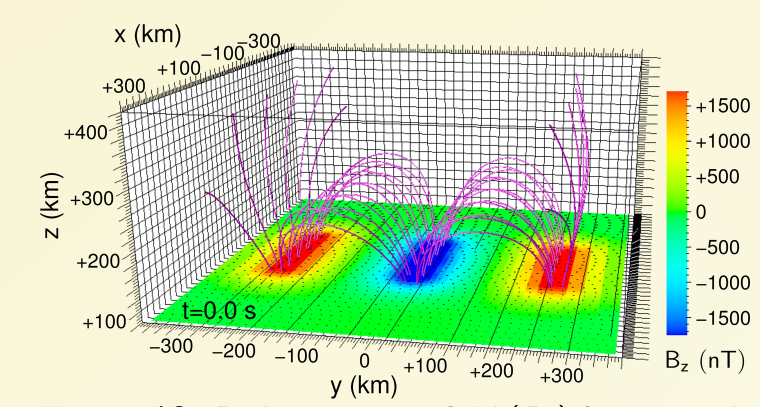

Figure 10: Radial magnetic field (B_z) for an arcade configuration. Solid magenta lines: magnetic field lines.

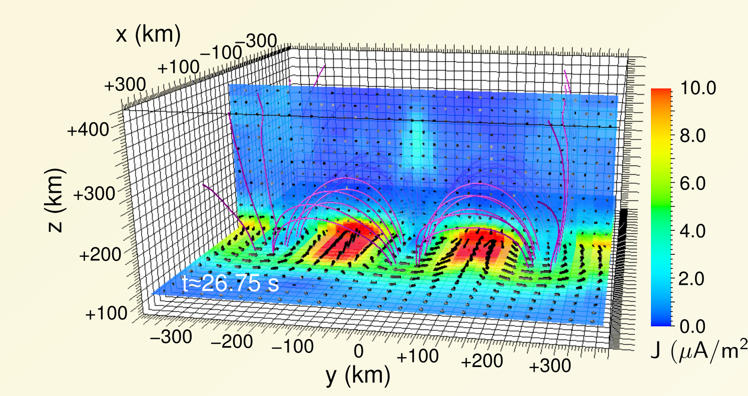

Figure 11: Magnitude (color map) and direction (solid black arrows) of the current density $\vec{J}$ in the planes y=0 km, and z=112 km. Solid magenta lines: magnetic field lines.

- The organized pattern of the modeled dynamo current is straightforwardly explained using magnetic dipoles & principle of superposition;
- A current is developing above the regions of converging field lines;
- Magnetic loops limit upward motion of particles.

Charge Carrier Dynamics

Figure 12: ▶ Charged particle flows above the dynamo region (through the 800×800 km^2-plane at z≈300 km): t (s) vs. F_i (#/s). Blue, red, and green lines: O_2^+, CO_2^+, and O^+ fluxes, respectively. Solid lines: magnetic cusp simulation. Dashed lines: magnetic arcade case.

$$F_i(z{=}300\ km) = \iint n_i \vec{V}_i \cdot \hat{z}\, dx\, dy$$

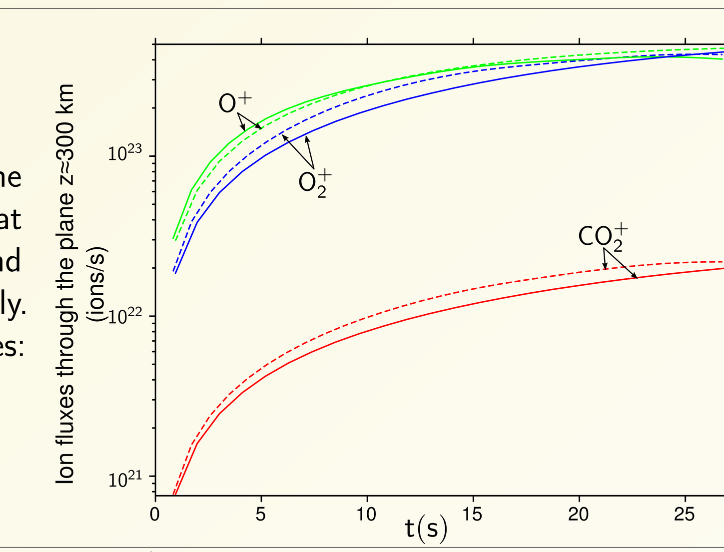

⇒ Strongly magnetized regions of Mars (e.g., Terra Sirenum) can efficiently shield the local atmosphere and alter the motion of charged particles from the lower to the upper atmosphere.

V. Conclusions

The principal results and contributions following from this work can be summarized as follows:
1. The dynamo current forms in a torus shape around the base of an isolated magnetic cusp due to the $\vec{E} \times \vec{B}$-drift of electrons;
2. The asymmetry in the horizontal component of the electric field is explained by the dependence of $\vec{E}$ on the collision-driven ion dynamics;
3. The organized pattern of the dynamo current produced by a striped magnetic field topology can be straightforwardly explained using the results from isolated vertically oriented, upward and downward magnetic dipoles, and the principle of superposition.
4. Strongly magnetized regions of Mars (e.g., Terra Sirenum) can efficiently shield the local atmosphere and alter the motion of charged particles from the lower to the upper atmosphere.

References

Brain, D. A., R. J. Lillis, D. L. Mitchell, J. S. Halekas, and R. P. Lin (2007), Electron pitch angle distributions as indicators of magnetic field topology near Mars, *J. Geophys. Res.*, *112*(A9), A09,201, doi:10.1029/2007JA012435.

Connerney, J. E. P., M. H. Acuña, N. F. Ness, G. Kletetschka, D. L. Mitchell, R. P. Lin, and H. Reme (2005), Tectonic implications of Mars crustal magnetism, *Proc. Natl. Acad. Sci. U.S.A.*, *102*(42), 14,970–14,975, doi:10.1073/pnas.0507469102.

Kopf, A. J., D. A. Gurnett, D. D. Morgan, and D. L. Kirchner (2008), Transient layers in the topside ionosphere of Mars, *Geophys. Res. Lett.*, *35*, L17102, doi:10.1029/2008GL034948.

Riousset, J. A., C. S. Paty, R. J. Lillis, M. O. Fillingim, S. L. England, P. G. Withers, and J. P. M. Hale (2013), Three-dimensional multifluid modeling of atmospheric electrodynamics in Mars' dynamo region, *J. Geophys. Res.*, *118*(6), 3647–3659, doi:10.1002/jgra.50328.

Riousset, J. A., C. S. Paty, R. J. Lillis, M. O. Fillingim, S. L. England, P. G. Withers, and J. P. M. Hale (2014), Electrodynamics of the Martian dynamo region near magnetic cusps and loops, *Geophys. Res. Lett.*, *41*(4), 1119–1125, doi:10.1002/2013GL059130.

This work was supported by the National Aeronautics and Space Administration under grant NNX10AM88G-MFRP to the Georgia Institute of Technology.